Environmental Processes (2021) 8:1455–1480
https://doi.org/10.1007/s40710-021-00537-9

ORIGINAL ARTICLE

Optimisation Approach Toward Water Management and Energy Security in Arid/Semiarid Regions

Danny M. Bajany[1] · Lijun Zhang[1] · Yongxin Xu[2] · Xiaohua Xia[1]

Received: 11 February 2021 / Accepted: 23 August 2021 / Published online: 7 September 2021

Abstract

This paper aims to develop, in a case of multiple water sources, an optimal operational strategy that can be used in arid/semiarid regions by water decision-makers to schedule the use of each source over time, to control the artificial recharge to aquifers, to improve the energy efficiency related to the water supply system, to determine the optimal amount of water each source should supply over a period, and to minimise the water costs. In this regard, a novel, cost effective, and advanced optimal controller to operate a water supply system in arid/semiarid regions has been developed. This model is designed as a multi-constraint non-linear programming model that meets the demand for an ever-growing population, and considers in its formulation multiple surface water sources, aquifers, desalination plants, recycled water plants, the seasonal availability of surface water and groundwater, the monthly rainfall variability, and the seasonal energy price. To verify the effectiveness of the developed model, a real case study was conducted. The results obtained showed a 3% reduction in the water supply cost and sustainable improvement in groundwater management, demonstrating the model's capacity to manage aquifer recharge efficiently, to optimally schedule the use of water sources. Adopting this strategy improves water security and the energy security in an urban region as it decreases the use of energy-intensive water sources during seasons with high electricity demand.

Keywords Water management · Modelling and optimisation · Energy security · Water resource scheduling · Water supply and demand

✉ Danny M. Bajany
dannybajany@gmail.com

[1] Department of Electrical, Electronic and Computer Engineering, University of Pretoria, Pretoria 0002, South Africa

[2] Department of Earth Sciences, University of Western Cape, Private Bag x17, Bellville 7535, South Africa

1 Introduction

Nowadays, planning, developing and managing water resources are vital to ensure adequate, cost-effective, and sustainable quality supply of water for both humans and natural ecosystems (Loucks and van Beek 2017). Indeed, water is a precious natural resource with limited availability. Approximately half of the world's potable water supply comes from rivers, either directly or from reservoirs (Barnett et al. 2005). With continuous population growth, the per capita availability of utilisable water is going down (Davijani et al. 2016; Abdulbaki et al. 2017; Zhou et al. 2017). Rapid industrialisation and urbanisation have led to an improved standard of living, increasing the demand for fresh water (Satiya et al. 2017). In addition, climate change has increased the weather variability and decreased the predictability of the rainfall in some regions which has resulted in shorter intervals between drought periods and made the natural water sources less reliable (Piao et al. 2010; Forsee and Ahmad 2011). Weather variability becomes a problem if one cannot get a couple of good years with above average rainfall, as this results in water stress in some regions (Xiong et al. 2010; Ebrahimi et al. 2021) and the need for water resource management. Managing freshwater resources under changing climatic conditions has become one of the important challenges facing modern global society (Vörösmarty et al. 2000; Oki and Kanae 2006; Piani et al. 2010). Hydrological variability coupled with fast-changing socio-economic boundary conditions have increased the uncertainties in water management and has led to the need for adaptive methods in water management (Ahmad and Simonovic 2001; Middelkoop et al. 2001; Mosquera-Machado and Ahmad 2007; Kalra and Ahmad 2011; Dawadi and Ahmad 2012). These methods would manage the transition from the current management regimes to more adaptive regimes that take into account environmental, human, technological, economic, institutional, and cultural characteristics of water sources (Pahl-Wostl 2007). These adaptive methods include optimal management and supply-side management, which are categorised according to the time horizon. The former is forward long-term planning while the latter is short-term planning (Hansen 2012). The importance of these adaptive methods is evidenced by the water crisis in Cape Town (South Africa) in 2015–2017. An optimal management strategy of water resources that can be applied to arid/semiarid regions is developed in this context.

In recent years, to cater to the freshwater deficit, some water-stressed regions have introduced alternative water sources such as seawater desalination, potable water recycling, and artificial aquifer recharge. This diversification of water sources has created a problem of allocating the use of these sources. The cost of water supplied differs from one source to another. The water demand varies seasonally, and the availability of surface water and groundwater sources is highly dependent on seasonal rainfall patterns (Shamshirband et al. 2020). Municipalities and other water decision-makers are facing the challenge of optimally allocating the use of each source seasonally across the planning horizon. Poor management in allocating these sources can result in higher water costs. The modelling and optimization approach proposed in this current work will address this challenge.

Various techniques in water supply optimisation which address the water allocation problem have been developed in the literature. An optimisation model for the conjunctive use of groundwater and surface water from a reservoir that considers reservoir decision rules, and detailed simulation of groundwater flow has been proposed (Belaineh et al. 1999). An optimisation model based on a genetic algorithm under a fuzzy environment to maximise

irrigation releases, hydropower production and level of satisfaction has also been developed (Regulwar and Raj 2009), and this model considers only reservoir decisions in its formulation. An optimisation model for allocating water resources was developed by Abdulbaki et al. (2017) to minimise the total water cost. The uniqueness of the model developed in Abdulbaki et al. (2017) lies in its ability to consider the spatially distributed water supply and demand nodes, and multiple water supply (seawater, surface, ground and wastewater) and demand types and qualities. Davijani et al. (2016) proposed a multi-objective socio-economic model to optimise the allocation of water resources to agriculture, industry, and municipal water sectors. Zhou et al. (2017) proposed a smart inter-basin water allocation methodology that allows for the establishment of optimal water allocation solutions under socio-economic development and mitigates the negative impacts of the inter-basin water transfer. Several mathematical models for the optimisation of the water irrigation allocation to maximise the economic benefit while satisfying the water demand and planted area constraints are presented in the literature (Kuo et al. 2000, 2003; Raju and Kumar 2004; Khare et al. 2006; Sahoo et al. 2006; Galán-Martín et al. 2015; Nguyen et al. 2017).

In addition, water and energy are inextricably linked and both are precious resources with limited availability (Wanjiru and Xia 2017; Kitessa et al. 2020; Wu et al. 2020). Water is needed for energy production and energy is needed for water production and supply (Sharif et al. 2019). Water supply systems are among the largest infrastructure assets of the industrial society (Sarbu 2016). Some researchers have indicated that 7% of the global energy is consumed for water distribution (Coelho and Andrade-Campos 2014). Water-related energy consumption can represent up to 12.6% of the national primary energy consumption (Sanders and Webber 2012). Energy security in countries amidst an electricity crisis can be severely affected due to the introduction of these alternative water sources. For instance, the introduction of seawater desalination, potable water recycling, network integration, and rainwater tanks during a decade of drought in South East Queensland (Australia) indicated an increase of 24% life cycle energy consumption of the existing water supply system (with surface water sources). Hence, this situation leads developing nations to seek for efficient energy demand management (Setlhaolo and Xia 2015; Nwulu and Xia 2015), water demand and supply management strategies (Cai et al. 2016), and efficient management strategies that co-ordinate the management of the two resources. Management of both resources together decreases the ancillary impact of one resource on the other (Engström et al. 2017). For this reason, several optimisation models have been developed in order to optimally analyse water and energy systems from a nexus approach under various sets of criteria (Li et al. 2018; Tsolas et al. 2018; Fuentes-Cortés et al. 2019a, 2019b; Oke et al. 2019; Mehrjerdi 2020). However, until now, to the best of the authors' knowledge, no work in the literature has conclusively dealt with the allocation problem of multiple water sources in arid/semiarid regions. The modelling and optimizations done to date do not simultaneously take into account the management of aquifer recharge, seasonal changes in electricity price, the availability of surface water and groundwater sources and at the same time incorporating rainfall patterns and water demand variations depending on climatic seasons as well as population growth. This paper deals with the aspects highlighted above.

The contribution of this study is the development of a novel optimal water resource management model which decision-makers can use to allocate the water resources in arid/semiarid regions with minimum cost and more sustainability. The developed model determines the optimal amount of water that each source should supply every period to meet the water demand, taking into account the parameters that affect the cost of water and the availability of

groundwater and surface water sources and also considering the time trend of the water demand. These parameters are the periodic and artificial recharge to the aquifer, the rainfall, the temperature, and the electricity price. The developed model avoids the fall of the aquifer water table because of its utilisation and keeps it in a state, allowing future users to use it as current users do. The model presented in this work will enable aquifers to recharge, return to their initial level, or even exceed it at the end of each year. Furthermore, the strategy developed ensures efficient use of the energy associated with the water supply system, allowing for a shift in the energy demand associated with the water supply system from on-peak season to off-peak season.

The paper is structured as follows: the first section gives a brief overview of the previous research; the second section presents the mathematical formulation of the developed optimisation model and the algorithm used to solve it; a case study is used in the third section to verify the effectiveness of the developed model, followed by the conclusions in the last section.

2 Mathematical Formulation

Figure 1 displays a water supply system that can get water from aquifers, surface water sources, desalination plants, and recycled water plants. This water supply system has two water distribution networks: one for recycled water and the other for potable water. The recycled water is only used for artificial recharge, industrial and irrigation purposes. In contrast, the surface water sources and aquifers can supply the demand for potable water and that for industrial and irrigation purposes. The desalination plant supplies water only to the distribution network for potable water. A part of the water pumped from aquifers returns to the aquifers after its utilisation by infiltration. There is also a quantity of water that is lost from the water distribution networks due to leaks.

2.1 Hydrology

The state equation of the aquifer y is given by the following equation (Hansen 2012):

$$H_{t+1}^{y} = \frac{R_t^y + (\alpha_t - 1) g_t^y}{A^y S^y} + H_t^y, \quad \alpha_t \in [0, 1], \tag{1}$$

where t is the index of the t_{th} month, y is the index of the y_{th} aquifer, H_{t+1}^{y} is the height in metres of the water table y at the end of the t_{th} period, g_t^y is the volume in cubic metres of water pumped from the water table y during the t_{th} period, R_t^y is the recharge to the y_{th} aquifer during the period t in cubic metres, α_t is the flow coefficient that measures the fraction of water pumped from a water table y that returns to the same water table. A^y and S^y are reservoir parameters: A^y is the geographic study area of concern in square metres covering the ground aquifer and S^y is the specific yield coefficient without units that measures the porous space where water exists in the water table aquifer y. H_t^y is the height in metres of the water table aquifer y at the beginning of the t_{th} month. Groundwater recharge occurs when water infiltrates at the land surface, flows through the unsaturated zone, and crosses the water table to enter the aquifer (Anderson et al. 2015). Temporal variations in recharge largely depend on climate and precipitation patterns (Fitts 2002). Several methods of measuring and estimating recharge, are

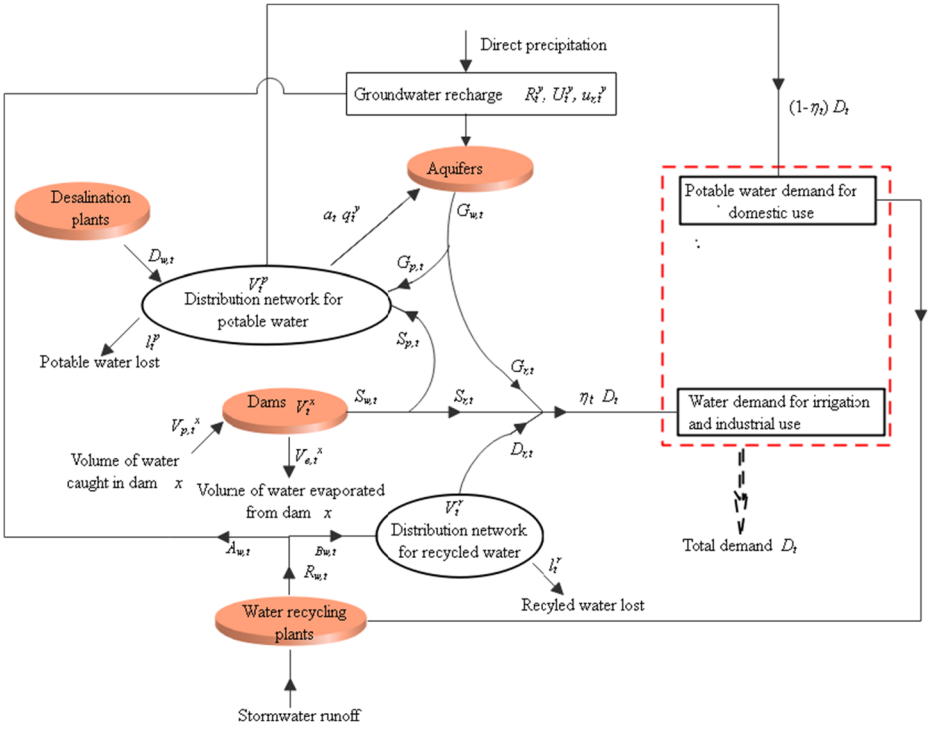

Fig. 1 Water supply system

largely discussed in Healy and Bridget (2010). Recharge can be expressed as a fraction of the local annual precipitation. For instance, the recharge of the Table Mountain aquifer in the Western Cape Province has been evaluated to vary between 1% and 55% of the mean annual precipitation (MAP) (Duah 2010). In the Western Cape Province, the major recharge source of aquifers is rainfall (Department of Water Affairs and Forestery 2008). However, artificial groundwater recharge is used to improve the efficiency of aquifers as the natural groundwater yield is insufficient to meet the long-term demand (Bugan et al. 2016). Artificial recharge is done with treated domestic wastewater blended with low-salinity urban runoff stormwater. Thus, R_t^y can be calculated as:

$$R_t^y = U_t^y + \sum_{r=1}^{R} u_{r,t}^y, \tag{2}$$

with U_t^y the recharge to the y_{th} aquifer due to the rainfall (direct precipitation) during the t_{th} period, R the total number of water recycling plants in the region, r the index of the r_{th} water recycling plant, and $u_{r,t}^y$ the water from the wastewater treatment plant r used to recharge the y_{th} aquifer during the t_{th} period.

2.2 Dynamics of Water Balance

Water balance is defined as the cumulative differences between net supply and demand (Zarghami and Akbariyeh 2012). Water balance is determined in the recycled water distribution network and the potable water distribution network as indicated in Eqs. (3) and (4),

respectively, by the groundwater, surface water, desalinated water, recycled water, water loss, and water demand:

$$V_{t+1}^{r} = V_{t}^{r} + \sum_{r=1}^{R} z_{t}^{t} - l_{t}^{r} - D_{r,t}, \tag{3}$$

$$V_{t+1}^{p} = V_{t}^{p} + \sum_{x=1}^{M} s_{p,t}^{x} + \sum_{y=1}^{N} g_{p,t}^{y} + \sum_{d=1}^{De} Q_{t}^{d} - l_{t}^{p} - (1-\eta_{t})D_{t}, \tag{4}$$

where V_t^r and V_t^p are quantities of water in the recycled and potable water distribution networks, respectively, at the beginning of the t_{th} month, V_{t+1}^r and V_{t+1}^p are volumes of water present in the recycled and potable water distribution networks, respectively, at the end of the t_{th} month or at the beginning of the $(t + 1)_{th}$ month. The second term in Eq. (3) represents the wastewater supplied by water recycling plants to the recycled water distribution network during the t_{th} month, z_t^r is the amount of water supplied to the recycled water distribution network by the r_{th} water recycling plant during the t_{th} month, l_t^r and l_t^p are the water losses from the recycled and potable distribution networks, respectively, in the t_{th} month, $D_{r,t}$ is the amount of water from the recycled water distribution network used for irrigation and industrial purposes during the t_{th} month. The second, the third and the fourth term in Eq. (4) represent the water supplied to the potable water distribution network from dams in the t_{th} month, the amount of groundwater supplied to the potable distribution network during the t_{th} month, and the water supplied in cubic metres from the desalinated water sources in the t_{th} month, respectively, x is the index of the x_{th}dam, $s_{p,t}^x$ is the amount of water supplied to the potable distribution network by the x_{th} dam during the t_{th} month, M is the total number of dams, $g_{p,t}^y$ is the amount of water supplied to the potable water distribution network by the y_{th} aquifer during the t_{th} month, N is the total number of aquifers, d is the index of the d_{th} desalination plant, Q_t^d is the amount of water supplied by the d_{th} desalination plant during the t_{th} month, De is the total number of desalination plants, D_t is the total volume of water in cubic metres allocated to the demands during the t_{th} period. Industrial demand, domestic demand, landscape demands, and other demands are the components of the total demand. η_t is a coefficient representing the percentage of the total water demand D_t used for irrigation and industrial purposes in the t_{th} month. η_t is determined from historical data of the water demand. The rate of leakage that can be managed is considered to be approximately 13% as in Zarghami and Akbariyeh (2012). Also:

$$s_{p,t}^{x} = s_{t}^{x} - s_{r,t}^{x}, \tag{5}$$

where s_t^x is the volume of water pumped from the dam x during the t_{th} sampling interval, and $s_{r,t}^x$ is the portion of s_t^x that is used for irrigation and industrial purposes, and.

$$z_{t}^{r} = q_{t}^{r} - \sum_{r=1}^{M} u_{r,t}^{y}, \tag{6}$$

where q_t^r is the volume of water supplied by the water recycling plant r during the t_{th} sampling interval.

2.3 Water Losses in Reservoirs by Evaporation

Water losses in dam x by evaporation ($V^x_{e,t}$) during the t_{th} period is computed from the average dam areas (Jain et al. 2005):

$$V^x_{e,t} = \left(a_i + a_f\right) e_t / 2, \tag{7}$$

where a_i and a_f are surface areas (m^2) at the beginning and the end of the period, and e_t is the evaporation depth (m) in the period t.

In South Africa, evaporation is measured at over 750 stations using the standard US Weather Bureau Class A (USWB Class A) evaporation pan. The USWB Class A evaporation pan is currently the most popular evaporation pan in usage, and it is universally adopted as the standard evaporation pan. To determine the daily evaporation, the change in water level from the previous day is recorded after taking into account the precipitation (Schulze and Maharaj 2006). Based on the data recorded from 570 South Africa stations, Schulze and Maharaj (2006) developed for each month a temperature-based equation of an A-pan equivalent evaporation for each of the 12 evaporation regions mapped in South Africa. The general form of the developed equation is given as follows:

$$e_t = b_0 T_{max} R_{a,t} + b_1 z - b_2 P_{md,t} + b_3 \tag{8}$$

where e_t is the A-pan equivalent reference evaporation estimate (mm/month), T_{max} is the monthly mean of daily maximum air temperature (°C), $R_{a,\,t}$ is the mean extra-terrestrial solar radiation for the month, z is the altitude (m), $P_{md,\,t}$ is the median monthly precipitation (mm), t is the month of the year and b_0-b_3 are regression constants.

2.4 Dynamics of Population

The demographic model that quantifies the anthropogenic influence of the current population, its expected changes, as well as the impact of population growth on water demand is expressed by Eq. (9) as:

$$D_j = P_j \, P_{cd,j}, \tag{9}$$

with:

$$P_j = P_0 \, e^{\delta j}, \tag{10}$$

and

$$P_{cd,j} = P_{cd,0} \, e^{\beta j}, \tag{11}$$

where P_0 is the initial population at the beginning of the time horizon, P_j is the expected population in year j, δ is the rate of population change based on past population growth rates with j the elapsed time (in years), $P_{cd,\,j}$ is the expected annual per capita demand, $P_{cd,\,0}$ is the initial annual per capita demand, β is the rate of per capita demand change. This exponent is obtained by inverting the exponential relationship to fit per capita demand in the last year of the time horizon. The per capita demand of water follows an exponential relationship based on the initial demand in the first year and that expected in the last year of the time horizon. The use of an exponential growth rate is based on the assertion by Kremer (1993) that an increase

in population would lead to an increase in technological change, driving water increase demand at a similar rate.

From Eqs. (9) and (11), the annual water demand D_j can be determined as: The water demand D_t of a specific month t is calculated in function of the annual demand as follows:

$$D_t = \gamma_t D_j \tag{12}$$

where γ_t is a coefficient representing the percentage of the annual water demand consumed in the month $t.\gamma_t$ of a specific month is determined from historical data of the monthly water demands of previous years.

2.5 Objective function

In this paper, four water sources are considered, namely: groundwater, surface water, desalinated water, and recycled water. The objective is to minimise the water cost by choosing among groundwater pumping, surface water, seawater desalination, and water recycling. This objective is subjected to the aquifer's equation of motion, surface water availability and future seasonal energy price projections. The aquifer must be kept in a state which allows prospective users to use it like current users while considering the impact of the seasonal hydro-climatic variables on the water demand and the increase of water demand due to population growth:

$$min \sum_{t=1}^{T} \left[\sum_{d=1}^{De} C_d\left(Q_t^d, \rho_t, t\right) + \sum_{y=1}^{N} C_g^y(H_t^y, g_t^y, \rho_t, t) + \sum_{x=1}^{M} C_s^x\left(s_t^x, \rho_t, t\right) + \sum_{r=1}^{R} C_r\left(q_t^r, \rho_t, t\right) \right] \tag{13}$$

where ρ_t is the electricity price during the t_{th} month, T is the total number of months that constitutes the time horizon, C_g^y is the cost of the water pumped from the aquifer y during the t_{th} sampling interval, C_s^x is the pumping cost of the water from the dam x, C_d is the cost of the supplied desalinated water during the t_{th} sampling interval, and C_r is the cost of the recycling water from the water recycling plant r.

The cost of the water pumped from an aquifer y is calculated as follows:

$$C_g^y(H_t^y, g_t^y, \rho_t, t) = \rho_t \, k \, g_t^y \left[\frac{R_t^y + (\alpha_t - 1) g_t^y}{A^y \, S^y} + H_t^y \right], \tag{14}$$

where k is a constant given by:

$$k = \frac{\rho_w \, g}{3.6 \times 10^6}, \tag{15}$$

with ρ_w the density of water [kg/m^3] and g the gravitational acceleration [$9.81 m/s^2$].

The costs of water from dams, desalination plants and water recycling plants during the t_{th} period are determined respectively by Eqs. (16), (17) and (18), as follows:

$$C_s^x\left(s_t^x, \rho_t, t\right) = \rho_t k_b q_t^x, \tag{16}$$

$$C_d\left(Q_t^d, \rho_t, t\right) = \rho_t\, k_d\, Q_t^d, \tag{17}$$

$$C_r\left(q_t^r, \rho_t, t\right) = \rho_t\, k_r\, q_t^r, \tag{18}$$

where: k_b, k_d and k_r are coefficients representing the amount of energy used for supplying one cubic metre of water from a surface water source, desalination plant, and water recycling plant, respectively.

2.6 Constraints

The volumes of water V_t^r and V_t^p in the distribution networks of the recycled water and that of potable water during every period t are constrained by:

$$V_{r,max} \geq V_t^r \geq V_{r,min}, \tag{19}$$

$$V_{p,max} \geq V_t^p \geq V_{p,min}, \tag{20}$$

where $V_{r,\,max}$ and $V_{p,\,max}$ represent the maximal volumes of water that can be stored in the reservoirs and pipes of the distribution networks of recycled and potable water, respectively, at every time t, $V_{r,\,min}$ and $V_{p,\,min}$ represent the minimal volumes of water in the distribution networks of recycled and potable water, respectively, that can prevent the outside untreated water from entering the pipes at the leak locations. Indeed, this could happen if the pipes are empty at the end of the sampling time.

The continuity of water supply in the recycled water distribution network must be ensured every time. This constraint is given by the water balance Eq. (3). Due to the dynamic demand of water for irrigation and industrial uses, Eq. (3) can be expressed as:

$$V_{h=t}^r = V_0^r + \sum_{h=0}^{t-1}\left[\sum_{r=1}^{R} z_h^r - l_h^r - D_{r,h}\right], \tag{21}$$

with:

$$h \in N | h = \{0, \ldots, t\}, \tag{22}$$

where V_0^r is the volume of water initially in the recycled water distribution network, and $V_{h=t}^r$ is the volume of water at the end of the t_{th} month in the recycled water distribution network.

The continuity of water supply in the potable water distribution network must be ensured every time. This constraint is given by the water balance Eq. (4). Due to the dynamic demand of potable water, Eq. (4) can be expressed as:

$$V_{h=t}^p = V_0^p + \sum_{h=0}^{t-1}\left[\sum_{x=1}^{M} s_{p,h}^x + \sum_{y=1}^{N} g_{p,h}^y + \sum_{d=1}^{De} Q_h^d - l_h^p - (1-\eta_h) D_h\right], \tag{23}$$

where V_0^p is the volume of water initially in the potable water distribution network, and $V_{h=t}^p$ is the volume of water at the end of the t_{th} month in the potable water distribution network. Equation (23) expresses the water balance at the t_{th} time interval as a function of the volume of water in the potable water distribution network at the beginning of the time horizon.

The total water supplied by aquifers, reservoirs, and recycled water plants for irrigation and industrial purposes should meet the no-potable water demand every month. This constraint is expressed as follows:

$$\sum_{y=1}^{N} g_{r,t}^{y} + \sum_{x=1}^{M} s_{r,t}^{x} + D_{r,t} = \eta_t D_t. \tag{24}$$

To prevent the water table from reaching a threshold level, the water table H_t^y is restricted by an h_{min}:

$$H_t^y \geq h_{min}. \tag{25}$$

Inequality (25) can also be written as:

$$\frac{R_t^y + (\alpha_t - 1) g_t^y}{A^y S^y} + H_t^y \geq h_{min}. \tag{26}$$

The dynamic variation of the height of the water table implies that inequality (26) can be written as shown by inequality (27):

$$H_0^y + \sum_{h=0}^{t-1} \frac{R_h^y + (\eta_h - 1) g_h^y}{A^y S^y} \geq h_{min}, \tag{27}$$

where H_0^y is the height of the water table y at the beginning of the time horizon.

To prevent the spillage of dams, the volume V_t^x of water in a dam x during each period t is restricted to the variation between a minimal volume V_{min}^x and a maximum volume V_{max}^x:

$$V_{min}^x \leq V_t^x \leq V_{max}^x \tag{28}$$

In discretised time, the dynamic variation of V_t^x can be determined as follows:

$$V_{t+1}^x = V_t^x + V_{p,t}^x - V_{e,t}^x - V_{q,t}^x, \tag{29}$$

or:

$$V_{h=t}^x = V_0^x + \sum_{h=0}^{t-1} \left(V_{p,h}^x - V_{e,h}^x - V_{q,h}^x \right), \tag{30}$$

with V_{t+1}^x the volume of water in the x_{th} dam at the end of the t_{th} time or at the beginning of the following time $t + 1$, V_0^x the volume of water initially in the x_{th} dam, $V_{e,t}^x$ the volume of water lost from dam x by evaporation during the t_{th} period, $V_{q,t}^x$ the volume of water pumped from the dam x during the t_{th} period, $V_{p,t}^x$ the volume of water caught in dam x due to the rainfall during the t_{th} period. V_t^x, V_{t+1}^x, $V_{p,t}^x$ and $V_{q,t}^x$ are expressed in cubic metres, $V_{p,t}^x$ for each period is calculated as follows:

$$V_{p.t}^x = 10^{-3} A_x \, \lambda_x, \tag{31}$$

where A_x is the catchment area in square metres for the dam x, namely the area from which rainfall flows into the dam x, and λ_t is the precipitation in millimetres during the t_{th} month.

To leave future users the capacity to function as well as the current users do, the aquifer level is constrained to be higher or equal to its initial level after each year. This constraint prevents the level of the aquifer from decreasing year to year due to its utilisation:

$$H_j^x \geq H_0^y \text{ with } j = 1, \ldots, J, \tag{32}$$

where j is the year index, H_j^y is the height of the water table y at the end of the j_{th} year, H_0^y is the height of the water table y at the beginning of the time horizon, and $J = T/12$ is the time horizon in years.

The water supplied by each recycled water plant and each desalination plant during each t_{th} period cannot exceed their capacities. This constraint is expressed by the following inequalities:

$$0 \leq q_t^r \leq RWP^r, \tag{33}$$

$$0 \leq Q_t^d \leq DWP^d, \tag{34}$$

where RWP^r and DWP^d are the capacities of the r_{th} recycled water plant and of the d_{th} desalination plant, respectively.

2.7 Algorithms

Several optimisation algorithms can be used to solve the nonlinear problem developed in this study. Since the water resource and energy optimisation problem has a nonlinear objective function, the "OPTI Toolbox" in MATLAB is used. This algorithm solves problems in this form:

$$\min f(X), \tag{35}$$

subject to:

$$\begin{cases} AX \leq b \quad (\textit{linear inequality constraint}) \\ AeqX = beq \ (\textit{linear equality constraint}) \\ C(X) \leq 0 \ (\textit{nonlinear inequality constraint}) \\ Ceq = 0 \ \ (\textit{nonlinear equality constraint}) \\ L_b \leq X \leq U_b \quad (\textit{lower and upper bounds}) \end{cases} \tag{36}$$

For the water resources and energy management model, the vector X contains the cost of water supplied by every source for all the months. The linear inequality constraints (19), (20), (28) and (32) are integrated into A and b and the linear equality constraints (21), (23) and (24) are integrated into Aeq and beq. The upper and lower boundary constraints (33) and (34) are incorporated into L_b and U_b.

3 Case Study and Data

3.1 Study Area and Context

The Western Cape Province is the third most populated province of South Africa after Gauteng and Kwazulu-Natal (Stats SA 2018). The province has a Mediterranean climate, with warm summers averaging a maximum of 26 °C, and a cool winter averaging a minimum of 7 °C (Olivier and Xu 2019). The majority of the annual rainfall occurs in winter, from June to August, while other seasons experience little rainfall. Analysis of precipitation data from 1841 to 2005 has indicated a mean annual rainfall of 619 mm (Adelana et al. 2006). However, in 2016 and 2017, only 221 mm and 154 mm of precipitation fell, respectively (CSAG 2020), which resulted in a lower level of water in dams. After the 2016 winter, dam levels were 15% lower than those expected at that period of the year. This situation led to the provincial government introducing a level-two water restriction (20% savings) (Olivier and Xu 2019) as the Western Cape water supply system relies predominantly on surface water, which entirely depends on rainfall. To cater for the water deficit caused by this drought and improve the reliability of the water supply system, the National Department of Water and Sanitation (NDWS) proposed the utilisation of additional water sources (City of Cape Town 2018). Among the responses advocated by the NDWS were the construction of a seawater desalination plant, the increase of groundwater pumping, and the increased capacity of the recycled water plant. These measures are not alien to the Western Cape (Sorensen 2017), however, the use of these alternative measures was negligible compared to surface water sources. For instance, only 2% of the water demand was covered by groundwater (City of Cape Town 2018), and 8% of domestic wastewater was recycled and reused for irrigation and industrial purposes (City of Cape Town 2018).

In the Western Cape Province, among all alternative water sources to surface water, groundwater abstraction is the most cost effective because of the presence of a number of aquifers (which include the Atlantis aquifer, the Cape Flats aquifer and the Table Mountain aquifer) (City of Cape Town 2018; Olivier and Xu 2019). The capital and operating costs related to groundwater abstraction are significantly lower than those of wastewater reuse and desalinated water because of the simplicity of the technology and the low energy required (City of Cape Town 2018). Groundwater abstraction cost is sensitive to water quality, borehole depth, yield and location. Groundwater abstraction plays a significant role in the Western Cape's water supply system. Due to the extreme drought, plans have been put in place to progressively increase its use from 12 to 100 million litres per day (City of Cape Town 2018; Olivier and Xu 2019).

However, in coastal aquifers such as in the Western Cape, excessive use of aquifers can result in salinity intrusion and ecological damage. To mitigate this risk, the Department of Water Affairs and Forestry (DWAF), with support from the Water Research Commission (WRC), has produced a strategy on artificial recharge, where surplus surface water is transferred underground to be stored in an aquifer for later abstraction or use (Department of Water and Sanitation 2017). Despite this strategy, some aquifers in the Western Cape have shown natural fluctuations in levels. Furthermore, groundwater recharge and the availability of surface water are highly dependent on seasonal rainfall patterns. Therefore, there is a need to monitor the fluctuation of the water tables and control the groundwater pumping, taking into account the recharge of aquifers. Groundwater pumping must be done to avoid excessive draw-down of the water tables and their dewatering, because their dewatering can modify the

soil water saturation and lead to disastrous consequences for agriculture and the environment. Thus, the strategy developed in this work will define an optimal pumping strategy to avoid the aquifers' dewatering and environmental damage. Irrespective of the water desalination process being expensive compared to other alternative water sources, the City of Cape Town (the biggest city in the Western Cape Province) is considering the development and commissioning of a permanent desalination plant with a capacity of 120 million litres per day (MLD) within the next five years to mitigate the water crisis due to the persistent drought. The desalination costs primarily depend on the scale, water salinity quality, temperature, marine works requirements, procurement methodology, and network integration costs. Water desalination is the most energy intensive among other options, having its energy cost evaluated to be double that needed for wastewater reuse (City of Cape Town 2018).

This diversification of water sources in the Western Cape has led to a problem in allocating the use of these sources. In the Western Cape Province, agriculture and tourism are major sources of income and are growing exponentially each year. Water represents an important catalyst and driver of socio-economic development. Poor management in allocating these resources will result in an expensive water cost, which can harm the growth of these two economic sectors. It may also hamper water access for the most vulnerable parts of the population.

3.2 Western Cape Water Supply System

The developed model was applied to the Western Cape Water Supply System (WCWSS) in South Africa. The WCWSS is a suitable case study because it can access water from dams, aquifers, water recycling plants, and desalination plants. The cost of water and the energy needed per thousand litres of water differ from one source to the another. The energy required for desalination (k_d) has been estimated to be twice that for recycled water (k_r), 3.5–4 kWh/m^3 and 2 kWh/m^3, respectively (City of Cape Town 2018). 1 kWh (k_b) is needed to supply one cubic metre of water from dams. In South Africa, the electricity tariff differs from winter to other seasons and increases annually. An electricity tariff of R 228.38 cents/kWh in winter, R 221.95 cents/kWh (1 Rand equals 0.067 US Dollars) in other seasons, and an annual electricity price increase of 5% are considered in this work.

The WCWSS has three aquifers and six major dams. The three aquifers are the Table Mountain aquifer (TM), the Cape Flats aquifer (CF), and the Atlantis aquifer (AT). The characteristics of aquifers and dams, aquifer recharge (U_t^1, U_t^2, and U_t^3) and the monthly precipitation (λ_t) were obtained from different governmental organisations (South African Department of Water Affairs and Forestry 2006; South African Weather Service 2020) and published articles (Adelana et al. 2010; Duah 2010; Jovanovic et al. 2017). Aquifer cover areas (A^1, A^2, and A^3), initial height (H_0^y) and their specific porous coefficient (S^y), the maximal capacities (V_{max}^1, V_{max}^2, V_{max}^3, V_{max}^4, V_{max}^5, and V_{max}^6) and catchment areas (A_1, A_2, A_3, A_4, A_5, and A_6) of dams are given in Table 1. The minimal volume of water admissible (V_{min}^x) in each dam x is fixed at 15% of its maximal capacity (V_{max}^x). The initial volume of water into the dams V_0^x is estimated to be 30% of their V_{max}^x.

Other assumptions and parameters used in the simulation are given in Table 2. In 2018, the population of the Western Cape Province was estimated at 6,025,888 and the annual rate of population change was estimated δ at 0.006 (Stats SA 2018). The annual per capita water demand was estimated at 92.76 [m^3/year/capita]. The monthly percentages (γ_t) of the annual

Table 1 Parameters used in the simulation

Characteristics	Notations	Values	Units
Aquifers			
Area of Table Mountain Aquifer	A^1	24,300,000	[m^2]
Area of Atlantis Aquifer	A^2	130,000,000	[m^2]
Area of Cape Flat Aquifer	A^3	630,000,000	[m^2]
Initial height of aquifers	H_0^y	25	[m]
Coefficient	S^y	0.02	
Dams			
Volume maximal of dam 1	V_{max}^1	$480{,}250 \times 10^3$	[m^3]
Volume maximal of dam 2	V_{max}^2	$164{,}122 \times 10^3$	[m^3]
Volume maximal of dam 3	V_{max}^3	$130{,}000 \times 10^3$	[m^3]
Volume maximal of dam 4	V_{max}^4	$58{,}644 \times 10^3$	[m^3]
Volume maximal of dam 5	V_{max}^5	$33{,}517 \times 10^3$	[m^3]
Volume maximal of dam 6	V_{max}^6	$31{,}767 \times 10^3$	[m^3]
Volume initial of water in dams	V_0^x	$30\% V_{max}^x$	[m^3]
Volume minimal of water admissible in dams	V_{min}^x	$15\% V_{max}^x$	[m^3]
Catchment area for dam 1	A_1	5×10^7	[m^2]
Catchment area for dam 2	A_2	30.608×10^7	[m^2]
Catchment area for dam 3	A_3	7.715×10^7	[m^2]
Catchment area for dam 4	A_4	2.96×10^6	[m^2]
Catchment area for dam 5	A_5	6.67×10^7	[m^2]
Catchment area for dam 6	A_6	2.17×10^7	[m^2]

water demand that represent the total monthly water demands (D_t), and the monthly percentages (η_t) of D_t that represent the monthly non-potable water demands were obtained from historical data provided by the Department of Water and Sanitation (2017). The flow coefficient α_t that measures the fraction of water pumped from an aquifer that returns to the same aquifer is assumed to be 8% of the water pumped from the considered aquifer. 13% of the water supplied by each source to the distribution network is lost due to the leakages. The monthly mean value of A-pan equivalent potential evaporation (e_t) for the Western Cape Province are those calculated by Eq. (8) (Schulze and Maharaj 2006). Artificial recharge is only practised at the Atlantis and Cape Flats aquifers.

3.3 Simulation Results and Discussion

The optimal scheduling of water sources utilisation obtained while using the developed water resource management model for a typical two year period is shown in Figs. 2, 3 and 4. Figure 2 shows the optimal quantity of water that each source supplies every month as a percentage of the monthly water demand D_t. For instance, in March of the first year, dam supply was 86%, aquifers 15%, desalination plant 6%, and the water recycling plant 8% of the D_t. The total quantity of water supplied by all sources represents 116% of the D_t in March. Figure 3 displays the quantity of water supplied by dams, aquifers and water recycling plants every month for irrigation and industrial uses as a percentage of the monthly non-potable water demand (MNPWD). For instance, in June of the first year, dams supplied 49%, aquifers 28%, and the recycled water distribution network supplied only 13% of the MNPWD. The water supplied by water recycling plants in June to the recycled distribution network represents 26% of the MNPWD. Lastly, Fig. 4 shows the quantity of water supplied by dams, aquifers, and the

Table 2 Parameters used in the simulation (continued)

Symbols	Units	Jan	Feb	Mar	Apr	May	Jun	Jul	Aug	Sep	Oct	Nov	Dec
e_t	[mm]	322	254	217	145	104	76	82	106	144	209	258	313
η_t		0.20	0.37	0.43	0.45	0.41	0.30	0.05	0.03	0.02	0.04	0.02	0.11
γ_t		0.08	0.12	0.13	0.12	0.12	0.09	0.06	0.05	0.05	0.05	0.06	0.07
λ_t	[mm]	15	17	20	41	69	93	82	77	40	30	14	17
U_t^1	[m^3]	335,340	128,304	330,966	1,669,410	3,611,466	3,452,544	2,165,130	2,681,262	3,090,960	593,406	478,224	624,024
U_t^2	[m^3]	296,400	1,201,200	780,000	1,482,000	4,851,600	6,068,400	2,886,000	4,680,000	2,823,600	187,200	405,600	1,404,000
U_t^3	[m^3]	854,000	646,800	1,016,400	2,525,600	5,328,400	6,342,000	3,026,800	4,776,800	4,569,600	543,200	708,400	1,867,600
Year 1 D_t	[m^3]	45,436,682	66,355,023	71,584,608	66,355,023	66,355,023	50,666,267	34,977,511	2,974,926	29,747,926	29,747,926	34,977,511	40,207,097
Year 2 D_t	[m^3]	46,191,997	67,487,995	72,811,995	67,487,995	67,487,995	51,515,996	35,543,998	30,219,998	30,219,998	30,219,998	35,543,998	740,867,997

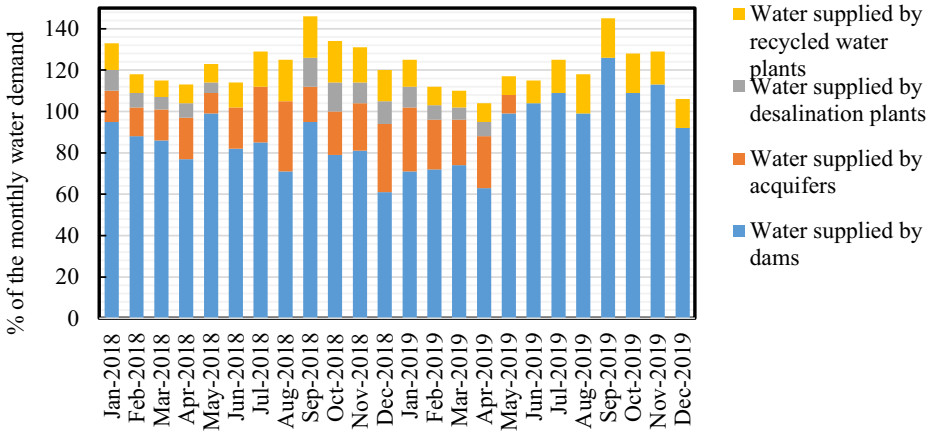

Fig. 2 Monthly water supply from each source as a percentage of the monthly water demand

desalination plant every month to the potable water distribution network as a percentage of the monthly potable water demand.

3.4 Monthly Cost of Water Supply

Figure 5 displays the trend of the monthly cost of water supply. It can be seen from this figure that the monthly cost of water from January to May of each year is relatively high compared to other months, with the highest cost in March. Water cost decreases gradually from June to August and reaches its minimum in August. From September to December, it increases and remains relatively low compared to the period from January to May. Indeed, the water demand is higher during the period from January to May while the rainfall is lower. Therefore, to meet the water demand, more water is pumped from dams during this period. The other sources are used to supply the deficit to avoid the water levels in dams reaching the limit of the non-brackish water supply. The period from June to August corresponds to the winter season, with lower water demand and higher rainfall. The amount of water in dams during this period is

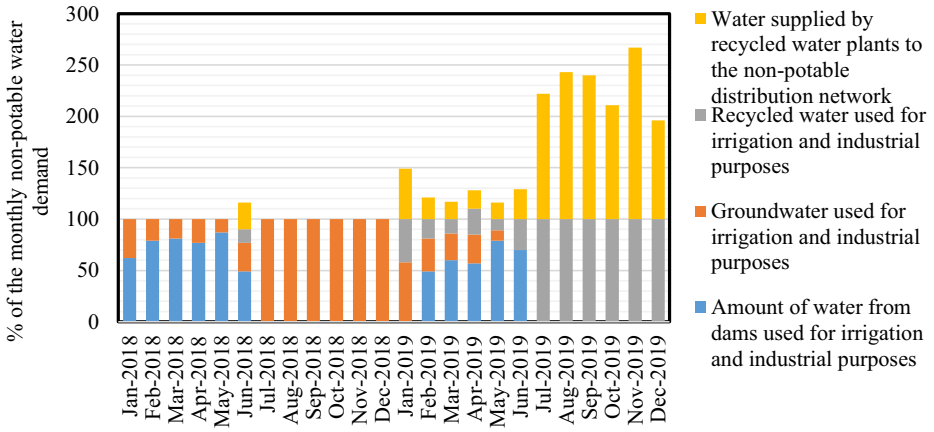

Fig. 3 Monthly water supply from dams, aquifers and recycled water plants for irrigation and industrial purposes as a percentage of non-potable water demand

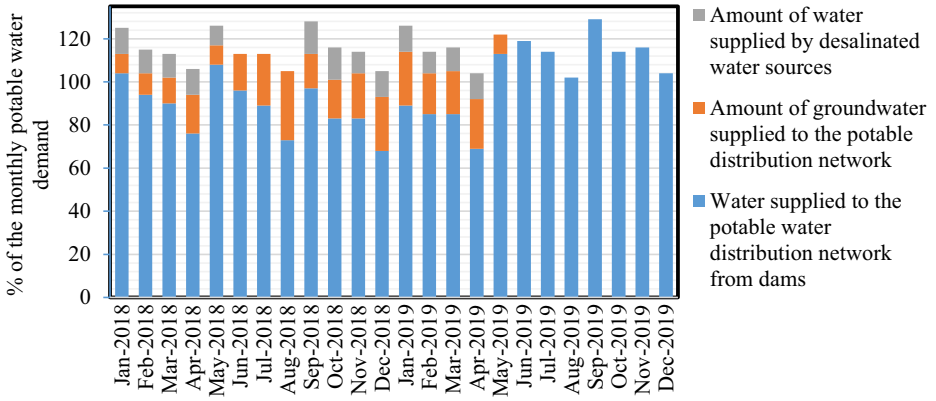

Fig. 4 Monthly water supply from dams, aquifers and desalination plants to the potable water distribution network as a percentage of the monthly potable water demand

enough to meet the demand. The water level increases significantly and reaches its highest level at the end of August. Therefore, the backstop sources are less used during this period. These observations are shown in Fig. 6 and justify why the water levels in dams become lowest in the period from February to May and increase from June to August (see Fig. 7). During the period following winter, the period from September to December, priority is given to dams to supply the major part of the water demand as surface water availability is high.

The optimal scheduling of the water resources utilisation, as depicted in Fig. 6, shows that the desalination plant does not supply water in winter, and it is less utilised the second year. This result has two advantages: Firstly, it decreases the overall cost of energy used for water production. Indeed, the results obtained with the developed model show a 3% reduction in the cost of water production. This is so because the electricity price is higher in winter (the period from June to August) than in other seasons, and it is subject to increase by 5% the second year. The desalination process is the most energy-intensive process, followed by the recycled water plant, compared to the other two water sources. Thus, the use of the desalination plant in winter or its high utilisation the second year can increase the energy cost. Secondly, not using the desalination plant in winter is also beneficial for the company which supplies the electricity, as it shifts a considerable load from an on-peak season (winter) to off-peak season (other seasons).

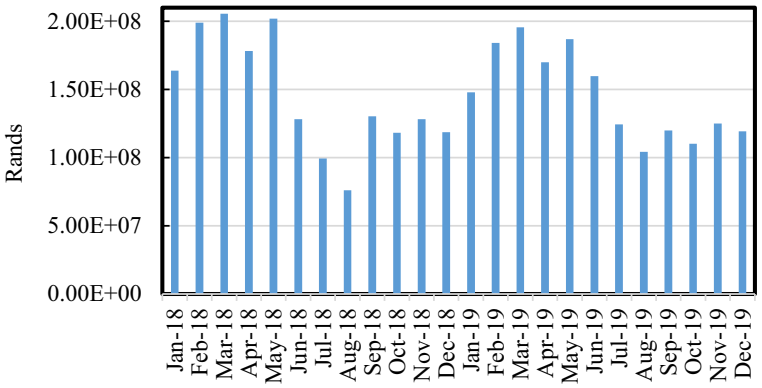

Fig. 5 Monthly cost of water supply

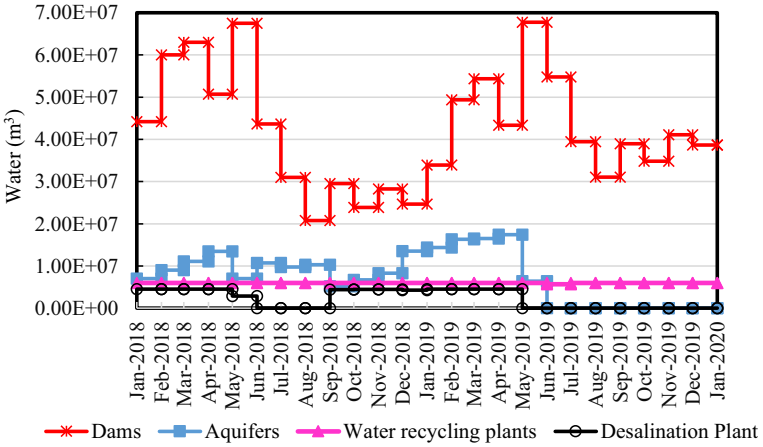

Fig. 6 Monthly water supplied by dams, aquifers, water recycling plants, and desalination plant

3.5 Water Trend in the Potable Water Distribution Network

Figure 8 displays the amount of water (V_t^p) at the end of each month in the potable water distribution networks (PWDN). The water levels in the distribution network fluctuate during the month. This is caused by fluctuations in water demand, which is managed by a consistent water supply that is continuously fed into the network and water reservoirs that act as buffers; this implies that the water in the distribution network is always renewed. The following observations are made: From January to March of the first year, a large reserve of water accumulates in the potable water distribution network despite a large consumption of drinking water during this period. This reserve of water comes mainly from dams. About 96% of the potable water demand (PWD) from January to March is supplied by dams. Aquifers and desalination plants supply 10% and 11% of the PWD respectively from January to March. The volume of water accumulated in the potable water distribution network supplements the water supplied by all the sources to meet the PWD in April. Indeed, in April, the PWD is higher than the water supplied by all the water sources minus the water losses, as displayed in Fig. 9. Thus,

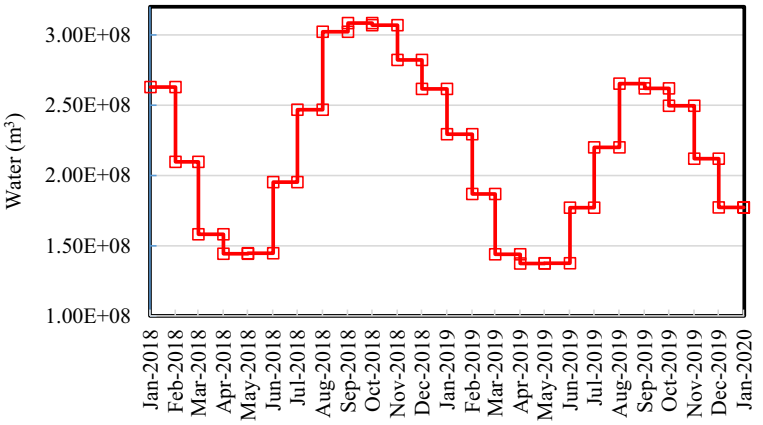

Fig. 7 The total amount of water available in dams

V_t^p declines significantly in April. In May, the water supplied by all the sources represents 124% of the D_t of May. A major part of supplied water is from dams. The water supplied by dams to the potable water distribution network represents 108% of the PWD. Aquifers and desalination plants each supply 9% of the PWD. Thus, the surplus of the supplied water is saved in the potable distribution network, which increases the V_t^p. The V_t^p in May, June and July is high whereas in the month of August it is low. In August, the total water supplied by dams and aquifers to the potable water distribution network cannot cover the water losses and meet the PWD, as shown in Fig. 9. Thus, to cover the losses and meet the PWD, the V_t^p of July supplements the water supplied by dams and aquifers. In September, October and November, the V_t^p is high, and in the month of December V_t^p is low. The total water supplied by all the sources in December is not enough to cover the losses l_t^p and the PWD. All the sources supply about 105% of the PWD while the l_t^p is about 13% of the water supply by all the sources. In the second year, similar observations can be made as for the first year.

3.6 Water Trend in the Recycled Water Distribution Network

Figure 10 displays the amount of water (V_t^r) at the end of each month in the recycled water distribution network (RWDN). From January of the first year to April of the second year, V_t^r remains at low level. During this period, the water supplied by water recycling plants covers the losses and the water consumed from the RWDN, as shown in Fig. 11. In May, the amount of water supplied to the RWDN is enough to cover the water consumed from it and the losses, and to increase the V_t^r. The V_t^r at the end of May supplements the water supplied by water recycling plants to meet the water consumed from the RWDN in June. Thus, V_t^r decreases significantly in June. From July until the end of November, V_t^rincreases gradually, as the water supplied by water recycling plants to the RWDN each month during this period is higher than the monthly water consumption and losses (see Fig. 11). The V_t^r at the end of November supplements the water supplied by water recycling plants to meet the water consumed from the RWDN in December.

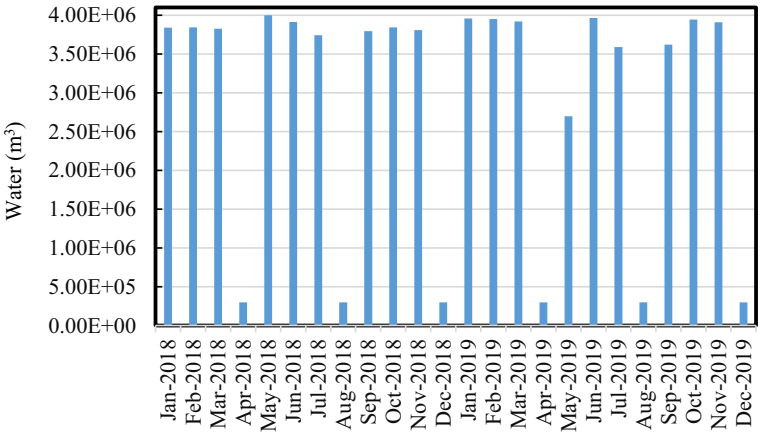

Fig. 8 Amount of water in the potable water distribution network at the end of each month

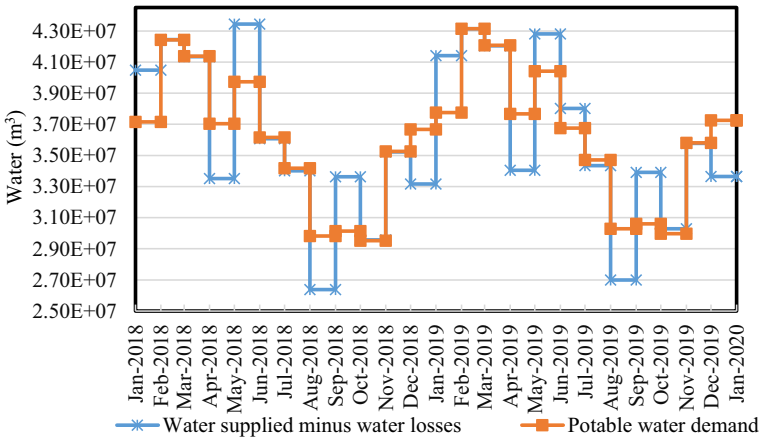

Fig. 9 Monthly water supply trend in the potable water distribution network and monthly potable water demand trend

3.7 Artificial Groundwater Recharge

Figure 12 displays the water supplied by water recycling plants for groundwater recharge. The main part of water supplied by water recycling plants in the first year is used for artificial groundwater recharge, which explains why the water table levels of aquifers are high throughout the first year (Fig. 13). In the second year, from January to June, the water recycling plants are less utilised for artificial groundwater recharge. The main part of the water from water recycling plants is sent into the non-potable water distribution network. During this period, the water demand is high, and groundwater is used extensively to meet the demand, which leads to a significant decrease in the level of aquifers (Fig. 13). From July to December, water recycling plants are highly utilised for artificial groundwater recharge to increase their levels. Thus, at the end of December of each year, the water table level of each aquifer is high or equals to their

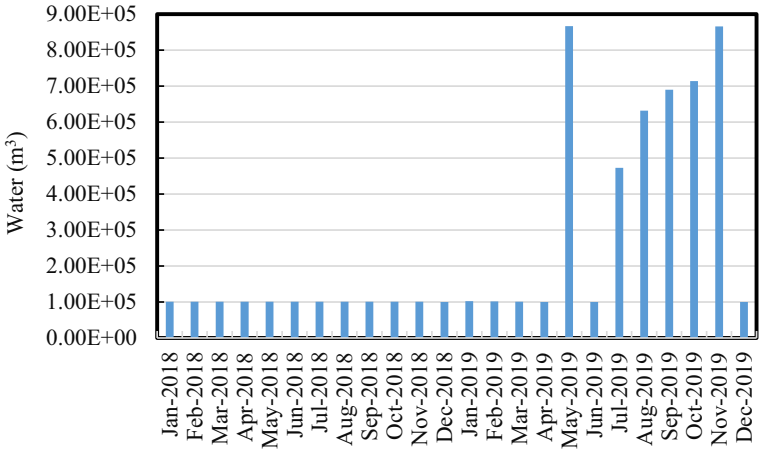

Fig. 10 Amount of water in the recycled water distribution network at the end of each month

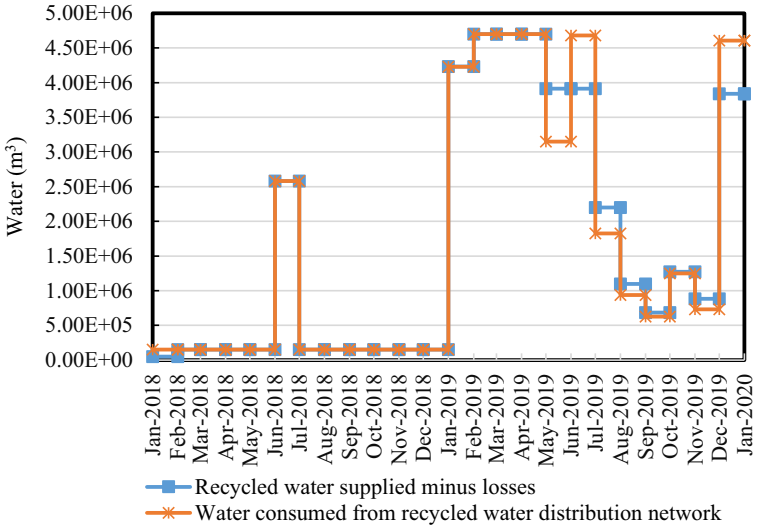

Fig. 11 Monthly water supply trend in the recycled water distribution network and monthly water consumed from the recycled water distribution network

initial levels. Therefore, using the developed water resource management strategy keeps aquifers in the same states, avoids their dry-out, and makes their utilisation sustainable. Figure 13 displays the variations of the water table levels of aquifers.

4 Conclusions

This paper introduces the first attempt to design a novel, cost-effective, and advanced optimal controller to operate a water supply system with multiple water sources in arid/semiarid regions. The developed strategy determines the optimal amount of water that each source

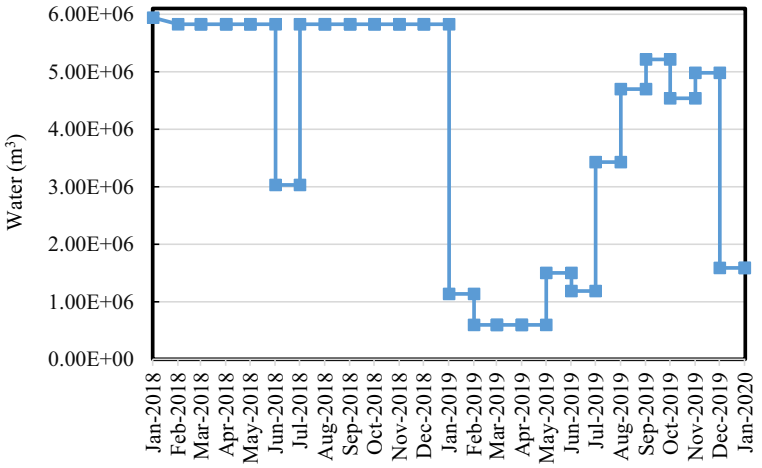

Fig. 12 Water supplied by water recycling plants for groundwater recharge

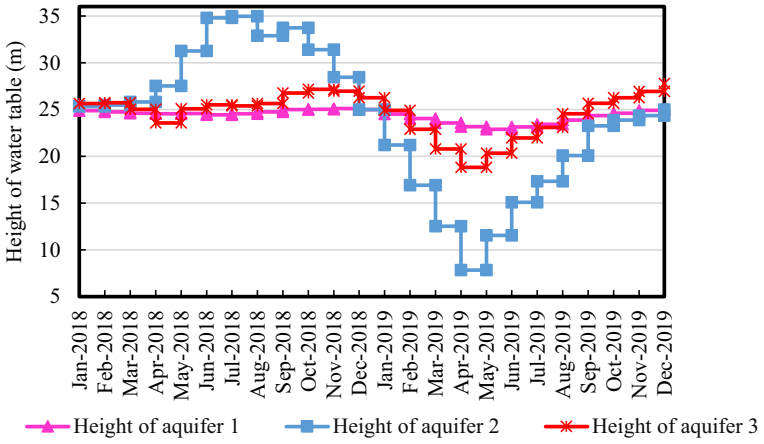

Fig. 13 Height of water tables

should supply every month while considering the availability of the source, the weather variability, the seasonal variation of the freshwater demand, as well as the seasonal and annual electricity price variation. The strategy also ensures efficient use of the energy associated with the system. The strategy developed herein allows for shifting of the energy demand associated with the water supply system from the on-peak season to the off-peak season. Furthermore, this model avoids the falling of water table and prevents it from drying out. It controls the aquifer recharge, allows aquifers to recharge, return to their initial levels, or exceed them at the end of each year. The use of the developed strategy makes the groundwater pumping more sustainable and enhances the planning efficiency of the pumping operations.

Although this strategy improves the management of water sources and makes the use of aquifers more sustainable as it allows aquifers to remain intact, it is only suitable when the water demand, the rainfall, the periodic recharge of aquifers, and temperature can be predicted accurately. However, this is not the case in practice. In practice, the water supply system is subject to external disturbances such as the dynamic variation of the weather prediction. Therefore, a management strategy that considers the dynamic variations of all parameters should be adopted as it is closer to reality. This reality will be addressed in future studies. In futures studies, diverse management strategies based on model predictive control strategies will be developed because of their predictive nature, ability to deal with disturbances and dynamic constraints inherent in the present problem.

Author Contributions **Danny Mpyana Bajany**: Conceptualisation, methodology, modelling, formal analysis, investigation, writing original draft preparation. **Lijun Zhang**: Conceptualisation, critical revision of the work, supervision. **Yongxin Xu**: Critical revision of the work, supervision. **Xiaohua Xia**: Critical revision, funding acquisition, supervision.

Funding The research leading to these results received funding from the Centre of New Energy System based at the University of Pretoria.

Data Availability All the data and software (custom code) used in this work are available to verify the result validity. They can be sent anytime requested.

Declarations

Ethical Approval We, authors Danny Mpyana Bajany, Prof Lijun Zhang, Prof Yongxin Xu and Prof Xiaohua Xia accept and certify that we have respected all ethical measures fixed by the Journal. We also declare that: this manuscript was not submitted to any other journal; this work is original and has not been published elsewhere in any form or language (partially or in full); the results are presented clearly, honestly and without fabrication and falsificafition; no data theories or text by others authors are presented as if they were ours. All data, text or theories by others authors have been acknowledged.

Consent to Participate This is not applicable.

Consent for Publication Not applicable.

Conflict of Interest We, authors Danny Mpyana Bajany, Prof Lijun Zhang, Prof Yongxin Xu and Prof Xiaohua Xia declare that we have no conflict of interest relevant to the content of this article.

References

Abdulbaki D, Al-Hindi M, Yassine A, Abou Najm M (2017) An optimization model for the allocation of water resources. J Clean Prod 164:994–1006. https://doi.org/10.1016/j.jclepro.2017.07.024

Adelana S, Xu Y, Adams S (2006) Identifying sources and mechanisms of groundwater recharge in the cape flats. Implications for Sustainable Resources Management, South Africa, pp 1–13

Adelana S, Xu Y, Vrbka P (2010) A conceptual model for the development and management of the cape flats aquifer, South Africa. Water SA 36:461–474. https://doi.org/10.4314/wsa.v36i4.58423

Ahmad S, Simonovic SP (2001) Integration of heuristic knowledge with analytical tools for the selection of flood damage reduction measures. Can J Civ Eng 28:208–221. https://doi.org/10.1139/cjce-28-2-208

Anderson MP, Woessner WW, Hunt RJ (2015) Applied groundwater modeling: simulation of flow and advective transport, 2nd edn. Academic Press, San Diego, California

Barnett TP, Adam JC, Lettenmaier DP (2005) Potential impacts of a warming climate on water availability in snow-dominated regions. Nature 438:303–309. https://doi.org/10.1038/nature04141

Belaineh G, Peralta RC, Hughes TC (1999) Simulation/optimization modeling for water resources management. J Water Resour Plan Manag 125:154–161. https://doi.org/10.1061/(ASCE)0733-9496(1999)125:3(154)

Bugan RDH, Jovanovic N, Israel S, Tredoux G, Genthe B, Steyn M, Allpass D, Bishop R, Marinus V (2016) Four decades of water recycling in Atlantis (Western cape, South Africa): past, present and future. Water SA 42:577–594. https://doi.org/10.4314/wsa.v42i4.08

Cai Y, Yue W, Xu L, Yang Z, Rong Q (2016) Sustainable urban water resources management considering life-cycle environmental impacts of water utilization under uncertainty. Resour Conserv Recycl 108:21–40. https://doi.org/10.1016/j.resconrec.2016.01.008

City of Cape Town (2018) Water Services and the Cape Town Urban Water Recycle. https://resource.capetown.gov.za/documentcentre/Documents/Graphics%5Cand%5Ceducational%5Cmaterial/Water%5C Services%5C and%5CUrban%5CWater%5CCycle.pdf. Accessed 14 Mar 2020

Coelho B, Andrade-Campos A (2014) Efficiency achievement in water supply systems-a review. Renew Sust Energ Rev 30:59–84. https://doi.org/10.1016/j.rser.2013.09.010

CSAG (2020) Current season's rainfall in Cape Town. http://www.csag.uct.ac.za/current-seasons-rainfall-in-Cape-Town/. Accessed 14 Mar 2020

Davijani MH, Banihabib ME, Anvar AN, Hashemi SR (2016) Multi-objective optimization model for the allocation of water resources in arid regions based on the maximization of socioeconomic efficiency. Water Resour Manag 30:927–946. https://doi.org/10.1007/s11269-015-1200-y

Dawadi S, Ahmad S (2012) Changing climatic conditions in the Colorado River basin: implications for water resources management. J Hydrol 430:127–141. https://doi.org/10.1016/j.jhydrol.2012.02.010

Department of Water Affairs and Forestery (2008) Groundwater maodel report Vol.5 Cape Flats aquifer model. https://www.dws.gov.za/Documents/Other/WMA/19/Reports/Rep9-Vol5-GWCape FlatsAquifer.pdf. Accessed 17 Aug 2021

Department of Water and Sanitation (2017) National Water and Sanitation Master Plan. http://www.dwa.gov.za/NationalWaterandSanitationMasterPlan/DocumentsReports.aspx. Accessed 28 Jul 2020

Duah AA (2010) Sustainable utilisation of Table Mountain Group aquifers. https://etd.uwc.ac.za/bitstream/handle/11394/2981/Duah_PHD_2010.pdf?sequence=1. Accessed 17 Aug 2021
Ebrahimi A, Rahimi D, Joghataei M, Movahedi S (2021) Correlation wavelet analysis for linkage between winter precipitation and three oceanic sources in Iran. Environmental Processes 8:1027–1045. https://doi.org/10.1007/s40710-021-00524-0
Engström RE, Howells M, Destouni G, Bhatt V, Bazilian M, Rogner H-H (2017) Connecting the resource nexus to basic urban service provision-with a focus on water-energy interactions in New York City. Sustain Cities Soc 31:83–94. https://doi.org/10.1016/j.scs.2017.02.007
Fitts CR (2002) Groundwater science. Elsevier
Forsee WJ, Ahmad S (2011) Evaluating urban storm-water infrastructure design in response to projected climate change. J Hydrol Eng 16:865–873. https://doi.org/10.1061/(ASCE)HE.1943-5584.0000383
Fuentes-Cortés LF, Flores-Tlacuahuac A, Ponce-Ortega JM (2019a) Integrated utility pricing and design of water-energy rural off-grid systems. Energy 177:511–529. https://doi.org/10.1016/j.energy.2019.04.026
Fuentes-Cortés LF, Ortega-Quintanilla M, Flores-Tlacuahuac A (2019b) Water-energy off-grid systems design using a dominant stakeholder approach. ACS Sustain Chem Eng 7:8554–8578. https://doi.org/10.1021/acssuschemeng.9b00348
Galán-Martín Á, Pozo C, Guillén-Gosálbez G, Antón Vallejo A, Jiménez Esteller L (2015) Multi-stage linear programming model for optimizing cropping plan decisions under the new common agricultural policy. Land Use Policy 48:515–524. https://doi.org/10.1016/j.landusepol.2015.06.022
Hansen JK (2012) The economics of optimal urban groundwater management in southwestern USA. Hydrogeol J 20:865–877. https://doi.org/10.1007/s10040-012-0841-7
Healy RW, Bridget RS (2010) Estimating groundwater recharge. Cambridge University Press, New York
Jain SK, Reddy N, Chaube UC (2005) Analysis of a large inter-basin water transfer system in India/analyse d'un grand système de transfert d'eau inter-bassins en Inde. Hydrol Sci J 50:137. https://doi.org/10.1623/hysj.50.1.125.56336
Jovanovic N, Bugan RDH, Tredoux G, Israel S, Bishop R, Marinus V (2017) Hydrogeological modelling of the Atlantis aquifer for management support to the Atlantis water supply scheme. Water SA 43:122–138. https://doi.org/10.4314/wsa.v43i1.15
Kalra A, Ahmad S (2011) Evaluating changes and estimating seasonal precipitation for the Colorado River basin using a stochastic nonparametric disaggregation technique. Water Resour Res 47. https://doi.org/10.1029/2010WR009118
Khare D, Jat MK, Ediwahyunan (2006) Assessment of counjunctive use planning options: a case study of Sapon irrigation command area of Indonesia. J Hydrol 328:764–777. https://doi.org/10.1016/j.jhydrol.2006.01.018
Kitessa BD, Ayalew SM, Gebrie GS, Teferi ST (2020) Quantifying water-energy nexus for urban water systems: a case study of Addis Ababa city. AIMS Environ Sci 7:486–504. https://doi.org/10.3934/environsci.2020031
Kremer M (1993) Population growth and technological change: one million BC to 1990. Q J Econ 108:681–716. https://doi.org/10.2307/2118405
Kuo S-F, Merkley GP, Liu C-W (2000) Decision support for irrigation project planning using a genetic algorithm. Agric Water Manag 45:243–266. https://doi.org/10.1016/S0378-3774(00)00081-0
Kuo S-F, Liu C-W, Chen S-K (2003) Comparative study of optimization techniques for irrigation project plannig. J Am Water Resour Assoc 39:59–73. https://doi.org/10.1111/j.1752-1688.2003.tb01561.x
Li Q, Yu S, Al-Sumaiti A, Turitsyn K (2018) Modeling and co-optimization of a Micro water-energy Nexus for smart communities. Proceedings - of the 2018 IEEE PES innovative smart grid technologies conference. https://doi.org/10.1109/ISGTEurope.2018.8571840
Loucks DP, van Beek E (2017) Water resource systems planning and management. Springer International Publishing, Cham
Mehrjerdi H (2020) Modeling and optimization of an island water-energy nexus powered by a hybrid solar-wind renewable system. Energy 197:117217. https://doi.org/10.1016/j.energy.2020.117217
Middelkoop H, Daamen K, Gellens D, Grabs W, Kwadijk JCJ, Lang H, Parmet BWAH, Schädler B, Schulla J, Wilke K (2001) Impact of climate change on hydrological regimes and water resources management in the Rhine basin. Clim Chang 49:105–128. https://doi.org/10.1023/A:1010784727448
Mosquera-Machado S, Ahmad S (2007) Flood hazard assessment of Atrato River in Colombia. Water Resour Manag 21:591–609. https://doi.org/10.1007/s11269-006-9032-4
Nguyen DCH, Ascough JC, Maier HR, Dandy GC, Andales AA (2017) Optimization of irrigation scheduling using ant colony algorithms and an advanced cropping system model. Environ Model Softw 97:32–45. https://doi.org/10.1016/j.envsoft.2017.07.002
Nwulu NI, Xia X (2015) Implementing a model predictive control strategy on the dynamic economic emission dispatch problem with game theory based demand response programs. Energy 91:404–419. https://doi.org/10.1016/j.energy.2015.08.042

Oke D, Mukherjee R, Sengupta D, Majozi T, El-Halwagi MM (2019) Optimization of water-energy nexus in shale gas exploration: from production to transmission. Energy 183:651–669. https://doi.org/10.1016/j.energy.2019.06.104

Oki T, Kanae S (2006) Global hydrological cycles and world water resources. Science 313:1068–1072. https://doi.org/10.1126/science.1128845

Olivier DW, Xu Y (2019) Making effective use of groundwater to avoid another water supply crisis in Cape Town, South Africa. Hydrogeol J 27:823–826. https://doi.org/10.1007/s10040-018-1893-0

Pahl-Wostl C (2007) Transitions towards adaptive management of water facing climate and global change. Water Resour Manag 21:49–62. https://doi.org/10.1007/s11269-006-9040-4

Piani C, Weedon GP, Best M, Gomes SM, Viterbo P, Hagemann S, Haerter JO (2010) Statistical bias correction of global simulated daily precipitation and temperature for the application of hydrological models. J Hydrol 395:199–215. https://doi.org/10.1016/j.jhydrol.2010.10.024

Piao S, Ciais P, Huang Y, Shen Z, Peng S, Li J, Zhou L, Liu H, Ma Y, Ding Y, Pierre F, Chunzhen L, Kun T, Yongqiang Y, Tianyi Z, Jingyun F (2010) The impacts of climate change on water resources and agriculture in China. Nature 467:43–51. https://doi.org/10.1038/nature09364

Raju KS, Kumar DN (2004) Irrigation planning using genetic algorithms. Water Resour Manag 18:163–176. https://doi.org/10.1023/B:WARM.0000024738.72486.b2

Regulwar DG, Raj PA (2009) Multi objective multireservoir optimization in fuzzy environment for river sub basin development and management. J Water Resour Prot 01(4):271–280. https://doi.org/10.4236/jwarp.2009.14033

Sahoo B, Lohani AK, Sahu RK (2006) Fuzzy multiobjective and linear programming based management models for optimal land-water-crop system planning. Water Resour Manag 20:931–948. https://doi.org/10.1007/s11269-005-9015-x

Sanders KT, Webber ME (2012) Evaluating the energy consumed for water use in the United States. Environ Res Lett 7:034034. https://doi.org/10.1088/1748-9326/7/3/034034

Sarbu I (2016) A study of energy optimisation of urban water distribution systems using potential elements. Water 8:593. https://doi.org/10.3390/w8120593

Satiya N, Varu V, Gadagkar A, Shaha D (2017) Optimization of water consumption using dynamic quota based smart water management system. IEEE Region 10 Symposium (TENSYMP), 2017 1–6. https://doi.org/10.1109/TENCONSpring.2017.8070075

Schulze RE, Maharaj M (2006) A-Pan equivalent reference potential evaporation. South African Atlas of Climatology and Agrohydrology, Water Research Commission, Pretoria, South Africa, WRC Report 1489:6

Setlhaolo D, Xia X (2015) Optimal scheduling of household appliances with a battery storage system and coordination. EnergyBuild 94:61–70. https://doi.org/10.1016/j.enbuild.2015.02.051

Shamshirband S, Hashemi S, Salimi H, Samadianfard S, Asadi E, Shadkani S, Kargar K, Mosavi A, Nabipour N, Chau KW (2020) Predicting standardized streamflow index for hydrological drought using machine learning models. Eng Appl Comput Fluid Mech 14:339–350. https://doi.org/10.1080/19942060.2020.1715844

Sharif MN, Haider H, Farahat A, Hewage K, Sadiq R (2019) Water–energy nexus for water distribution systems: a literature review. Environ Rev 27:519–544. https://doi.org/10.1139/er-2018-0106

Sorensen P (2017) The chronic water shortage in Cape Town and survival strategies. Int J Environ Stud 74:515–527. https://doi.org/10.1080/00207233.2017.1335019

South African Department of Water Affairs and Forestry (2006) Guidelines for water supply systems operation and management plans during Normal and drought conditions (RSA C000/00/2305), volume 2, appendix a: the Western cape water supply system pilot study. Pretoria

South African Weather Service (2020) Historical Rain. https://www.weathersa.co.za/home/historicalrain. Accessed 23 Mar 2020

Stats SA (2018) Department: statistics of South Africa, mid-year population estimates. In: Statistical release P. https://www.statssa.gov.za/publications/P0302/P03022019.pdf

Tsolas SD, Karim MN, Hasan MMF (2018) Optimization of water-energy nexus: a network representation-based graphical approach. Appl Energy 224:230–250. https://doi.org/10.1016/j.apenergy.2018.04.094

Vörösmarty CJ, Green P, Salisbury J, Lammers RB (2000) Global water resources: vulnerability from climate change and population growth. Science 289:284–288. https://doi.org/10.1126/science.289.5477.284

Wanjiru E, Xia X (2017) Optimal energy-water management in urban residential buildings through grey water recycling. Sustain Cities Soc 32:654–668. https://doi.org/10.1016/j.scs.2017.05.009

Wu W, Maier HR, Dandy GC, Arora M, Castelletti A (2020) The changing nature of the water–energy nexus in urban water supply systems: a critical review of changes and responses. J Water Clim Chang 11:1095–1122. https://doi.org/10.2166/wcc.2020.276

Xiong W, Holman I, Lin E, Conway D, Jiang J, Xu Y, Li Y (2010) Climate change, water availability and future cereal production in China. Agric Ecosyst Environ 135:58–69. https://doi.org/10.1016/j.agee.2009.08.015

Zarghami M, Akbariyeh S (2012) System dynamics modeling for complex urban water systems: application to the city of Tabriz, Iran. Resour Conserv Recycl 60:99–106. https://doi.org/10.1016/j.resconrec.2011.11.008
Zhou Y, Guo S, Hong X, Chang F-J (2017) Systematic impact assessment on inter-basin water transfer projects of the Hanjiang River basin in China. J Hydrol 553:584–595. https://doi.org/10.1016/j.jhydrol.2017.08.039